The capacity change of a bounded object in a parallel plate capacitor

Gerhard Kristensson
Dept. of Electrical and Information Technology, Lund University, P.O. Box 118, SE-221 00 Lund, Sweden.
Gerhard.Kristensson@eit.lth.se

Abstract

The change in capacitance, if an object is introduced in a parallel plate capacitor, is analyzed. The integral representation of the potential is exploited in a systematic way to solve the potential everywhere inside the capacitor. In particular, the change in capacitance is extracted. The method shows similarities with the null field approach to solve dynamic problems.

1 Background

The motivation to revisit an electrostatic problem is easily found in the newborn interest in quantifying the static electric and magnetic properties of an object, *i.e.*, its polarizability dyadics $\boldsymbol{\gamma}_{\rm e}$ and $\boldsymbol{\gamma}_{\rm m}$. The reason for this attention is that the broadband properties of a scatterer, an antenna or a periodic structure stated as sum rules, are determined by the values of these dyadics [1–3, 7–9]. As an example, for a finite scatterer, we have that

$$\int_0^\infty \frac{\sigma_{\rm ext}(k)}{k^2}\,{\rm d}k = \frac{\pi}{2}\left(\hat{\boldsymbol{e}}^*\cdot\boldsymbol{\gamma}_{\rm e}\cdot\hat{\boldsymbol{e}} + (\hat{\boldsymbol{k}}_{\rm i}\times\hat{\boldsymbol{e}})^*\cdot\boldsymbol{\gamma}_{\rm m}\cdot(\hat{\boldsymbol{k}}_{\rm i}\times\hat{\boldsymbol{e}})\right)$$

which shows that the extinction cross section of the object, $\sigma_{\rm ext}(k)$, as a weighted integral over the wave number k (*i.e.*, proportional to the frequency), depends directly on the static electric and magnetic polarizability dyadics $\boldsymbol{\gamma}_{\rm e}$ and $\boldsymbol{\gamma}_{\rm m}$. The polarization of the incident plane wave is denoted $\hat{\boldsymbol{e}}$, and the incident direction of the plane wave is $\hat{\boldsymbol{k}}_{\rm i}$.

The polarizability of an object quantifies the induced disturbance due to an external, homogeneous, static electric field. If we aim at extracting the polarizability from an experimental setup that employs a parallel plate capacitor,[1] the influence of the higher modes, which are inevitably present due to fact that the exciting sources are located at a finite distance from the object, has to be mastered. In this paper, we exploit a solution technique which has had its main success in solving time harmonic problems in geometries that contain both infinite and bounded surfaces. In particular, the solution of scattering of buried objects has been solved with this technique [6].

2 The formulation of the problem

The geometry of the problem is shown in Figure 1. Two infinite, perfectly conducting planes, S_1 and S_2, parameterized by $z = z_i$ = constant, $i = 1, 2$, confine the volume V_4 (labeled region 4 in the figure), which also excludes the object under test in volume V_3 (region 3), bounded by the surface S_3. For simplicity, in this paper we assume that the object in volume V_3 is a perfectly conducting object, *i.e.*, the potential Φ on its surface is then a constant, which we denote by Φ' (at the moment unknown). The potential $\Phi(\boldsymbol{r})$ satisfies the Laplace equation in volume V_4, and the appropriate scalar boundary value problem to solve in this paper becomes

$$\begin{cases} \nabla^2\Phi(\boldsymbol{r}) = 0, \quad \boldsymbol{r}\in V_4 \\ \Phi(\boldsymbol{r}) = \Phi_i, \quad \boldsymbol{r}\in S_i, \quad i=1,2 \\ \Phi(\boldsymbol{r}) = \Phi', \quad \boldsymbol{r}\in S_3 \end{cases} \tag{1}$$

At large lateral distances the potential is $\Phi(\boldsymbol{r}) = \left(\Phi_2(z-z_1) - \Phi_1(z-z_2)\right)/d$, where the distance between the plates is $d = z_2 - z_1$. The potentials Φ_1 and Φ_2 are given (excitation of the problem).

[1] This experiment is reported in another paper presented at this conference.

978-1-4244-6051-9/11/$26.00

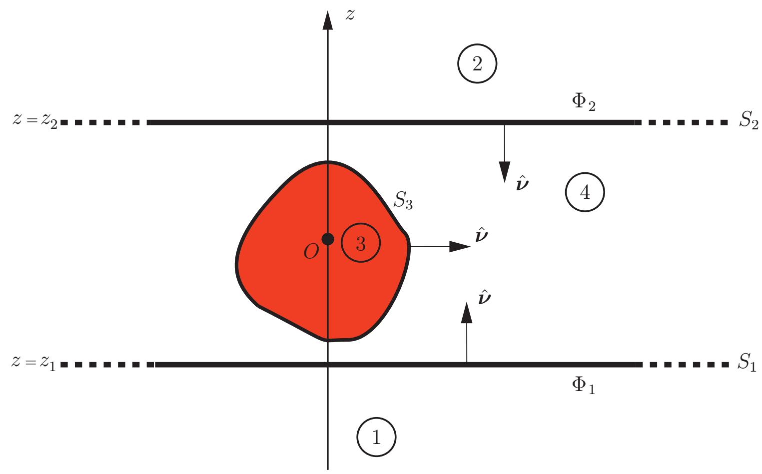

Figure 1: The geometry of the capacity problem with the two confining surfaces S_1 and S_2 and the object under test bounded by S_3.

3 Solution

The integral representation of the potential is the starting point of the analysis [10]. With the directions of the unit normals on S_i, $i = 1, 2, 3$ in Figure 1, the solution of the problem in (1) satisfies the following integral relations:

$$-\sum_{i=1}^{3} \iint_{S_i} \frac{\hat{\boldsymbol{\nu}}(\boldsymbol{r}') \cdot \nabla' \Phi(\boldsymbol{r}')}{4\pi |\boldsymbol{r} - \boldsymbol{r}'|} \, \mathrm{d}S' = \begin{cases} \Phi_1, & \boldsymbol{r} \text{ in region 1} \\ \Phi_2, & \boldsymbol{r} \text{ in region 2} \\ \Phi', & \boldsymbol{r} \text{ in region 3} \\ \Phi(\boldsymbol{r}), & \boldsymbol{r} \text{ in region 4} \end{cases} \tag{2}$$

To obtain the solution of the potential problem, we have to eliminate the unknown surface fields, $-\hat{\boldsymbol{\nu}} \cdot \nabla\Phi$, in the integrals in (2). This is accomplished by the same technique as solving time harmonic problems in similar geometries [6]. The position vector, $\boldsymbol{r}$, can take four different principle positions. In three of them, region 1, 2, and 3, we obtain relations between the unknown surface fields on S_3, and on S_i, $i = 1, 2$. The forth region, region 4, is used to find an expression of the induced field in region 4.

The solution includes the solution to an infinite system of equations, that contains the influence of all higher modes. No details of the solution is presented here, but we refer to a technical report for details [5]. The system of equations are

$$c_n = 4\pi\delta_{n,\mathrm{e}01} + \sum_{n'n''} \frac{P_{nn''} T_{n''n'}}{d^{l+l''+1}} c_{n'} \tag{3}$$

where the matrix $P_{nn'}$ is independent of the distance $d = z_2 - z_1$, the distance between the plates. For $z_2/d = 1/2$, it explicitly given as

$$P_{nn'} = N_{nn'} \frac{(l+l')!}{2^{l+l'+1}} \zeta(l+l'+1, 1) \left(1 + (-1)^{l+l'}\right) \left(\left(2^{l+l'+1} - 1\right) - (-1)^{l+m}\right)$$

where $\zeta(z)$ is the Riemann zeta function, and the normalization constants are

$$N_{nn'} = \frac{\delta_{m,m'} \delta_{\sigma,\sigma'}}{\sqrt{(l+m)!(l-m)!(l'+m)!(l'-m)!}}$$

The transition matrix, $T_{nn'}$, characterizes the object bounded by S_3 completely [11]. Algorithms to find this matrix are found in the literature [5, 11]. We solve this system (3) for c_n.

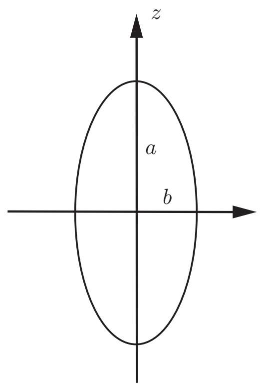

Figure 2: The geometry of the spheroid with half axes a and b, respectively.

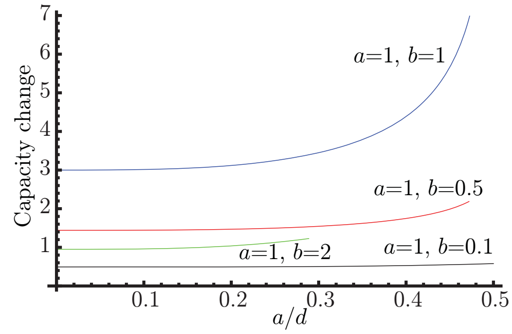

Figure 3: The capacity changed in (4) (scaled by the volume of the circumscribing sphere) of a perfectly conducting spheroid as a function of the ratio a/d. The curves have ratios $a/b = 0.1, 0.5, 1, 2$, depicted as black, red, blue, and green curves, respectively.

The quantity of interest in this paper is the change of capacity due to the introduction of the object bounded by S_3 inside the plates. The planes — equally but opposite charged — and the body carries no net charge. The capacity change, in terms of the transition matrix, $T_{nn'}$, and the array c_n, is [5]

$$\frac{\Delta C d^2}{\epsilon_0} = \sum_n T_{\mathrm{e}01n} c_n \tag{4}$$

4 Numerical simulations

An interesting and important test object is the spheroidal geometry, see Figure 2. The change in capacitance $\Delta C d^2/\epsilon_0$ in (4) (scaled by the volume of the circumscribing sphere) for a set of spheroids is depicted in Figure 3. The exact value of the polarizability γ_{zz} is [4]

$$\gamma_{zz} = \frac{4\pi a b^2}{3L_3}$$

where the depolarization factor L_3 is

$$L_3 = \begin{cases} \dfrac{1-e^2}{2e^3}\left(\ln\dfrac{1+e}{1-e} - 2e\right) & \text{(prolate)} \\ \dfrac{1}{e^2}\left(1 - \dfrac{\sqrt{1-e^2}}{e}\arcsin e\right) & \text{(oblate)} \end{cases}$$

and the eccentricity $e = \sqrt{1-\xi^2}$, where $\xi = \min\{a/b, b/a\} \in [0,1]$ is the ratio between the minor and the major semi-axes of the spheroid. For the sphere, $e = 0$, we get $L_3 = 1/3$, and $\gamma_{zz} = 4\pi a^3$.

The second example of test objects is the cylindrical geometry, see Figure 4. The change in capacitance $\Delta C d^2/\epsilon_0$ in (4) (scaled by the volume of the circumscribing sphere) for a set of cylinders is depicted in Figure 5.

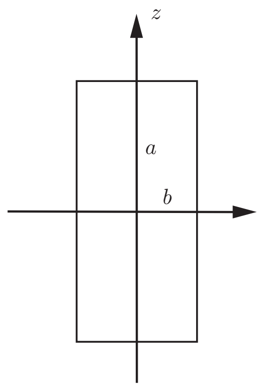

Figure 4: The geometry of the cylinder with height $2a$ and diameter $2b$, respectively.

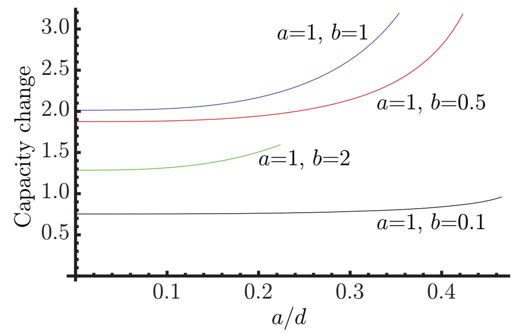

Figure 5: The capacity changed in (4) (scaled by the volume of the circumscribing sphere) of a perfectly conducting cylinder as a function of the ratio a/d. The curves have ratios $a/b = 0.1, 0.5, 1, 2$, depicted as black, red, blue, and green curves, respectively.

References

[1] M. Gustafsson and D. Sjöberg. Physical bounds and sum rules for high-impedance surfaces. Technical Report LUTEDX/(TEAT-7198)/1–17/(2010), Lund University, Department of Electrical and Information Technology, P.O. Box 118, S-221 00 Lund, Sweden, 2010. `http://www.eit.lth.se`.

[2] M. Gustafsson and D. Sjöberg. Sum rules and physical bounds on passive metamaterials. *New Journal of Physics*, **12**, 043046, 2010.

[3] M. Gustafsson, C. Sohl, and G. Kristensson. Illustrations of new physical bounds on linearly polarized antennas. *IEEE Trans. Antennas Propagat.*, **57**(5), 1319–1327, May 2009.

[4] R. C. Jones. A generalization of the dielectric ellipsoid problem. *Phys. Rev.*, **68**(3–4), 93–96, 1945.

[5] G. Kristensson. The polarizability and the capacity change of a bounded object in a parallel plate capacitor. Technical Report LUTEDX/(TEAT-7203)/1–39/(2010), Lund University, Department of Electrical and Information Technology, P.O. Box 118, S-221 00 Lund, Sweden, 2010. http://www.eit.lth.se.

[6] G. Kristensson and S. Ström. Scattering from buried inhomogeneities — a general three-dimensional formalism. *J. Acoust. Soc. Am.*, **64**(3), 917–936, 1978.

[7] C. Sohl, M. Gustafsson, and G. Kristensson. Physical limitations on broadband scattering by heterogeneous obstacles. *J. Phys. A: Math. Theor.*, **40**, 11165–11182, 2007.

[8] C. Sohl, M. Gustafsson, and G. Kristensson. Physical limitations on metamaterials: Restrictions on scattering and absorption over a frequency interval. *J. Phys. D: Applied Phys.*, **40**, 7146–7151, 2007.

[9] C. Sohl, C. Larsson, M. Gustafsson, and G. Kristensson. A scattering and absorption identity for metamaterials: experimental results and comparison with theory. *J. Appl. Phys.*, **103**(5), 054906, 2008.

[10] S. Ström. Introduction to integral representations and integral equations for time-harmonic acoustic, electromagnetic and elastodynamic wave fields. In V. V. Varadan, A. Lakhtakia, and V. K. Varadan, editors, *Field Representations and Introduction to Scattering*, volume 1 of *Handbook on Acoustic, Electromagnetic and Elastic Wave Scattering*, chapter 2, pages 37–141. Elsevier Science Publishers, Amsterdam, 1991.

[11] P. C. Waterman. Matrix methods in potential theory and electromagnetic scattering. *J. Appl. Phys.*, **50**(7), 4550–4566, 1979.